

A Kinetic Model for Vapor-liquid Flows

Aldo Frezzotti, Livio Gibelli and Silvia Lorenzani

*Dipartimento di Matematica del Politecnico di Milano
Piazza Leonardo da Vinci 32 - 20133 Milano - Italy*

Abstract. The evaporation of a liquid slab into vacuum is studied by numerical solutions of the Enskog-Vlasov equation for a fluid of spherical molecules interacting by Sutherland potential. The main aim of this work is to obtain the structure of the vapor-liquid interface in non-equilibrium conditions as well as the distribution function of evaporating molecules. The results show that the distribution function of molecules crossing a properly defined vapor-liquid boundary is almost Maxwellian and that the vapor phase is reasonably well described by the Boltzmann equation with diffusive boundary condition.

INTRODUCTION

In many situations of great theoretical and practical interest it is necessary to study the motion of a vapor in contact with its condensed phase. Most studies of evaporation/condensation phenomena adopt kinetic theory methods and focus on the behavior of the vapor phase[1]. Accordingly, the bulk of the condensed phase is often assigned fixed properties and the structure of the vapor-liquid(solid) interface is reduced to a surface Σ bounding the vapor. Molecular exchanges through Σ are modelled by the following inhomogeneous linear boundary condition for the distribution function $f(\bar{\mathbf{x}}, \mathbf{v}|t)$ of molecular velocities \mathbf{v} at a location $\bar{\mathbf{x}}$ on Σ :

$$(\mathbf{v} \circ \mathbf{n})f(\bar{\mathbf{x}}, \mathbf{v}|t) = (\mathbf{v} \circ \mathbf{n})f_e(\mathbf{v}) + \int_{(\mathbf{v}_1 \circ \mathbf{n}) < 0} R(\mathbf{v}, \mathbf{v}_1) |\mathbf{v}_1 \circ \mathbf{n}| f(\bar{\mathbf{x}}, \mathbf{v}_1|t) d^3\mathbf{v}_1, \quad \mathbf{v} \circ \mathbf{n} > 0 \quad (1)$$

Eq.(1) states that the molecular flux emerging from a surface element of normal unit vector \mathbf{n} has two components. The first one consists of the molecules initially belonging to the condensed phase and evaporating into the vapor phase with distribution function $f_e(\mathbf{v})$, the second one of vapor molecules whose initial velocity \mathbf{v}_1 is instantaneously changed to \mathbf{v} by the interaction with the condensed phase, described by the scattering kernel $R(\mathbf{v}, \mathbf{v}_1)$. The usual choice for the distribution function $f_e(\mathbf{v})$ of molecules evaporating from the condensed phase is the half range Maxwellian

$$f_e(\mathbf{v}) = \sigma_e \frac{n_w}{(2\pi RT_w)^{3/2}} \exp\left(-\frac{\mathbf{v}^2}{2RT_w}\right), \quad \mathbf{v} \circ \mathbf{n} > 0 \quad (2)$$

being n_w the number density of the saturated vapor at the temperature T_w , whereas Maxwell's gas-surface scattering kernel is the usual choice to describe molecular re-emission from the condensed phase:

$$R(\mathbf{v}, \mathbf{v}_1) = (1 - \sigma_e) \left[\alpha (\mathbf{v} \circ \mathbf{n}) \frac{1}{2\pi(RT_w)^2} \exp\left(-\frac{\mathbf{v}^2}{2RT_w}\right) + (1 - \alpha) \delta(\mathbf{v} - \mathbf{v}_1 + 2(\mathbf{v}_1 \circ \mathbf{n})\mathbf{n}) \right] \quad (3)$$

The evaporation coefficient σ_e ($0 \leq \sigma_e \leq 1$) gives the fraction of vapor molecules impinging on the interface and absorbed. The total fraction of impinging molecules which are *instantaneously* re-emitted is $1 - \sigma_e$, α being the probability of diffuse re-emission and $1 - \alpha$ the probability of specular reflection. The assessment of the model accuracy and/or the determination of the model parameters requires either difficult experiments or theoretical tools capable of describing both phases.

In the present work the evaporation of a fluid into vacuum is studied by the Enskog-Vlasov equation[2, 3, 4]. This kinetic equation describes a dense fluid whose molecules interact via an intermolecular potential which is splitted into a hard core, treated as in standard Enskog equation, and an attractive tail that enters the equation linearly in a mean field term

Report Documentation Page				Form Approved OMB No. 0704-0188	
Public reporting burden for the collection of information is estimated to average 1 hour per response, including the time for reviewing instructions, searching existing data sources, gathering and maintaining the data needed, and completing and reviewing the collection of information. Send comments regarding this burden estimate or any other aspect of this collection of information, including suggestions for reducing this burden, to Washington Headquarters Services, Directorate for Information Operations and Reports, 1215 Jefferson Davis Highway, Suite 1204, Arlington VA 22202-4302. Respondents should be aware that notwithstanding any other provision of law, no person shall be subject to a penalty for failing to comply with a collection of information if it does not display a currently valid OMB control number.					
1. REPORT DATE 13 JUL 2005		2. REPORT TYPE N/A		3. DATES COVERED -	
4. TITLE AND SUBTITLE A Kinetic Model for Vapor-liquid Flows				5a. CONTRACT NUMBER	
				5b. GRANT NUMBER	
				5c. PROGRAM ELEMENT NUMBER	
6. AUTHOR(S)				5d. PROJECT NUMBER	
				5e. TASK NUMBER	
				5f. WORK UNIT NUMBER	
7. PERFORMING ORGANIZATION NAME(S) AND ADDRESS(ES) Dipartimento di Matematica del Politecnico di Milano Piazza Leonardo da Vinci 32 - 20133 Milano - Italy				8. PERFORMING ORGANIZATION REPORT NUMBER	
9. SPONSORING/MONITORING AGENCY NAME(S) AND ADDRESS(ES)				10. SPONSOR/MONITOR'S ACRONYM(S)	
				11. SPONSOR/MONITOR'S REPORT NUMBER(S)	
12. DISTRIBUTION/AVAILABILITY STATEMENT Approved for public release, distribution unlimited					
13. SUPPLEMENTARY NOTES See also ADM001792, International Symposium on Rarefied Gas Dynamics (24th) Held in Monopoli (Bari), Italy on 10-16 July 2004. , The original document contains color images.					
14. ABSTRACT					
15. SUBJECT TERMS					
16. SECURITY CLASSIFICATION OF:			17. LIMITATION OF ABSTRACT UU	18. NUMBER OF PAGES 6	19a. NAME OF RESPONSIBLE PERSON
a. REPORT unclassified	b. ABSTRACT unclassified	c. THIS PAGE unclassified			

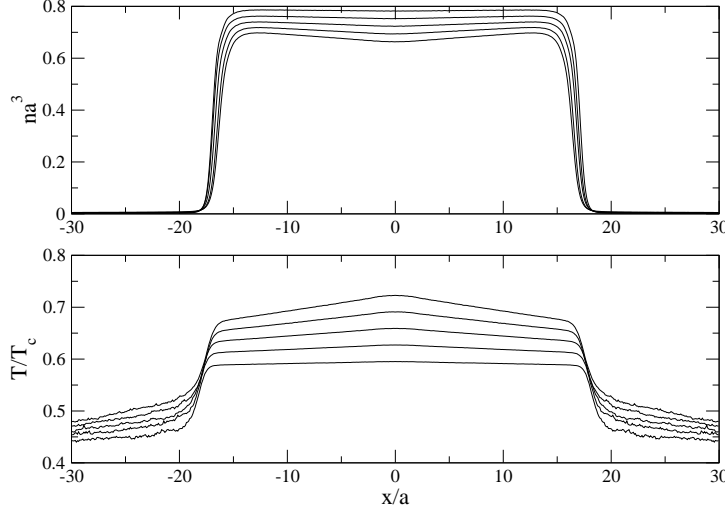


FIGURE 1. (a) Density profiles and (b) Temperature profiles for $T/T_c = 0.596, 0.663, 0.729, 0.795, 0.862$.

$$\frac{\partial f_1}{\partial t} + \mathbf{v} \circ \nabla_{\mathbf{x}} f_1 + \frac{1}{m} \left(\int_{\|\mathbf{x}_1 - \mathbf{x}\| > a} \frac{d\phi}{dr} \frac{\mathbf{x}_1 - \mathbf{x}}{\|\mathbf{x}_1 - \mathbf{x}\|} n(\mathbf{x}_1|t) d\mathbf{x}_1 \right) \circ \nabla_{\mathbf{v}} f_1 = C_E(f_1, f_1) \quad (4)$$

being $\phi(r)$ the Sutherland potential and $C_E(f_1, f_1)$ the Enskog collisional integral.

Eq.(4) provides a simplified description of the microscopic behavior of the fluid but it has the capability of handling both the liquid and vapor phases, thus eliminating the necessity of postulating *ad hoc* models for boundary conditions at the vapor-liquid interface.

EVAPORATION INTO VACUUM: NUMERICAL RESULTS AND DISCUSSION

The behavior of the distribution function f_e of the molecules initially in the liquid phase and entering the vapor region through the vapor-liquid interface has already been obtained in previous MD studies of evaporation/condensation phenomena[5, 6], and deviations from the Maxwellian behavior have been reported. However, in the MD simulations cited above it was necessary to adopt some criterion to distinguish the contribution of f_e from the contribution of vapor molecules entering the condensed phase and reflected back to the vapor region after a short time interaction with the interface molecules. In this work the unwanted contribution of reflected vapor molecules is minimized by placing a perfectly absorbing planar wall, close and parallel to the vapor-liquid interface[7, 8]. The distance between the wall and the interface is much smaller than the mean free path in the gas phase so that most molecules leave the liquid surface and hit the absorbing wall without suffering intermediate collision, but larger than a few molecular diameters, in order to avoid interferences with the formation of the interface. A particle scheme[9] has been used to calculate approximate solutions of Eq(4). The spatial domain is a finite symmetric interval $[-L/2, L/2]$ of the x axis with two perfectly absorbing walls located at the boundary $x = \pm L/2$. Each computation is started by arranging a homogeneous liquid slab at temperature T_L in the center of the computational domain. The progressive cooling of the system is avoided by thermostating[10] at constant temperature T_L a thin strip, $4a$ wide, in the central part of the slab.

The net evaporation flow causes the consumption of the liquid slab and the slow movement of the vapor-liquid interfaces. Left to itself, the resulting flow would be unsteady and the possibility of computing macroscopic quantities by time averaging in the poorly populated vapor region would be lost. However, it should be observed that the velocity of the interface is much smaller than the characteristic vapor velocity, at temperatures well below T_c , hence the flow will be quasi steady. To limit the interface motion and use time averaging of flow properties, the following procedure has been adopted. After the initial transient dies out, time averaging of system properties is performed over a short time interval. During this time, the motion of the interface is negligible. At the end of this time interval, the interfaces are reset in their original position by translating the fluid particles in each domain towards the closest absorbing wall. The thin empty gap, created in the center of the slab by particles translation, is filled with the particles absorbed at the

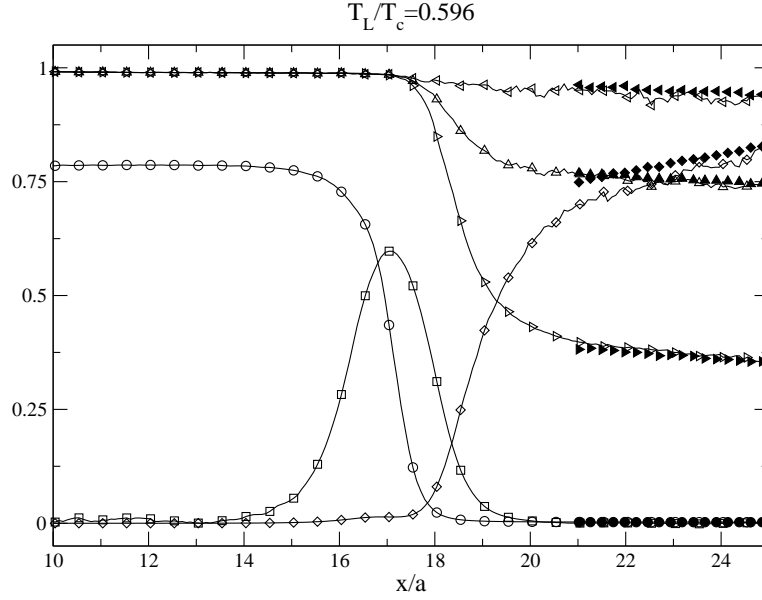


FIGURE 2. Non-equilibrium profiles in the vapor-liquid interface region; \circ , number density na^3 ; \triangleleft , normalized transversal temperature T_{\perp}/T_L ; \triangleright , normalized longitudinal temperature T_{\parallel}/T_L ; \triangle , normalized overall temperature T/T_L ; \diamond , normalized velocity $u_x/\sqrt{RT_L}$; \square , mean field $-1/10F_x a/(RT_L)$; filled symbols: DSMC Boltzmann equation solution with diffusive boundary condition at $x = x_m$.

walls; their new random velocities are generated by sampling a Maxwellian with temperature T_L . Since the gap width equals the sum of interfaces displacements during the averaging time interval, the density in the center of the slab keeps its equilibrium constant value. At the end of the translation the fluid motion is again calculated and time averaging continues. The results obtained by the method outlined above have been successfully compared with a simpler, but much more time consuming, method in which interfaces are free to move and the unsteady flow properties are obtained from the superposition of a few hundreds independent program runs.

Simulations have been performed in a relatively narrow temperature range. The lower temperature limit is given by the necessity of keeping the liquid density within the validity range of the Carnahan-Starling approximation and keeping the vapor density high enough for significant statistics. The higher temperature limit is given by the request of having a dilute vapor phase. Density profiles are shown in Fig.1(a). Each density profile has a minimum in the center of the slab and two local maxima in proximity of the interfaces because the evaporation cooling of the slab causes a temperature decrease and a density increase in the external region of the liquid slab. The corresponding temperature profiles are shown in Fig.1(b). The central thermostated strip keeps the prescribed temperature value T_L . In the liquid bulk, temperature profiles exhibit an almost linear trend whose slope is more pronounced for the highest temperature values. Temperature profiles suffer a sudden drop in the interface regions, but the rate of temperature change rapidly diminishes in the vapor region. The small, but evident, temperature gradient in the gas phase indicates that the effect of collisions in the gas phase is not completely negligible.

The non-equilibrium structure of the interface is outlined in Fig. 2, where density, mean field F_x and mean velocity u_x are shown along with the profiles of transversal (T_{\perp}), longitudinal (T_{\parallel}) and total temperature $T = (T_{\perp} + 2T_{\parallel})/3$. The results show that T_{\perp} , T_{\parallel} and T follow the same almost linear behavior not only in the bulk of the liquid phase but also in the interface region. The three curves separate at a position x_s where the density amounts to about 25% of its maximum value. This separation position marks the beginning of a transition layer which extends a few molecular diameters into the low density region. This layer is characterized by the action of the mean field F_x whose effects are still felt at a distance of about $3a$ from the center of the interface, defined as the point x_c where the density takes the value $(n_l + n_g)/2$. After the separation position, T_{\perp} is almost constant and the structure of the transition layer is better shown by T_{\parallel} whose rapid drop follows the increase of u_x . As shown by the sudden decrease in their rate of change, the velocity u_x and the longitudinal temperature T_{\parallel} complete their transition to the dilute gas regime at a distance x_m of about $4a$ from the interface center. As discussed below in greater detail, this is the position x_m where the matching with Boltzmann equation solutions should be done and the boundary condition applied.

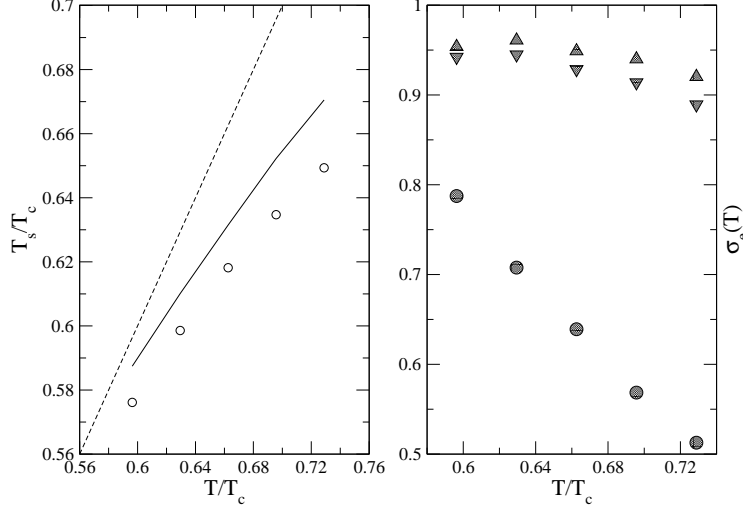


FIGURE 3. (a) Temperature at the separation location as a function of T_L . Solid line, T_s from numerical solutions of Eq.(4); \circ , T_s from Eq.(6); (b) Evaporation coefficient σ_e as a function of T_L . \circ , σ_e from $n_g(T_L)$; ∇ , σ_e from $n_g(T_s)$; \triangle , σ_e from $n_g(T_s)$ and back scattered flux correction.

The behavior of T_s , the temperature value at x_s , as a function of T_L is shown in Fig.3(a). The separation temperature T_s increases more slowly than T_L because the evaporation cooling becomes more and more important as T_L grows. In the explored temperature range, the temperature difference $T_L - T_s$ exhibits a linear dependence from the mass flux J_m . The above results suggest a simple but approximate method to calculate T_s by assuming that the temperature field in the liquid slab center up the separation point can be described by the classical heat transport equation. Accordingly, at the separation point the following relationship holds:

$$-\chi(T_s) \left(\frac{dT}{dx} \right)_{x_s} = (\Delta E) J_m \quad (5)$$

where $\chi(T_s)$ is the heat conductivity and ΔE is the total energy per particle carried away from the liquid phase by evaporation through an imaginary surface located at x_s . Since the flow is quasi stationary and the temperature field is close to a linear function of x , the boundary condition (5) can be turned into the following equation for T_s

$$T_L - T_s = \frac{x_s}{\chi(T_s)} \Delta H \sigma_e n_g(T_s) \sqrt{\frac{RT_s}{2\pi}} \quad (6)$$

by approximating $\frac{dT}{dx}$ with $(T_s - T_L)/x_s$, ΔE with the latent heat of vaporization ΔH and J_m with $\sigma_e n_g(T_s) \sqrt{\frac{RT_s}{2\pi}}$. The heat conductivity $\chi(T)$ is not affected by the attractive tail[3], hence it can be computed from its Enskog theory approximation[11]. As shown in Fig.3(a), Eq.(6) slightly underestimates T_s , but reproduces the correct behavior as T_L is changed.

EVAPORATION COEFFICIENTS AND DISTRIBUTION FUNCTIONS

Simulations results show that, after an initial transient, the particles flux at the absorbing wall reaches a constant value J_m which can be used to estimate the evaporation coefficient σ_e . It should be observed that the net particles flux J_m at the wall underestimates the true evaporating flux \tilde{J}_m because a few evaporating particles are scattered back toward the interface by collisions. However, in the conditions under examination, the applied correction does not exceed 2%. The calculation of σ_e requires a reference Maxwellian flux which can be obtained either from T_L or from some other reference temperature that can be attributed to the evaporating liquid surface. It is not clear how a specific temperature value can be assigned to the liquid surface in the present non-equilibrium conditions, however the temperature T_s is also a reasonable choice as a reference temperature, since it takes into account the effects of evaporation cooling and it

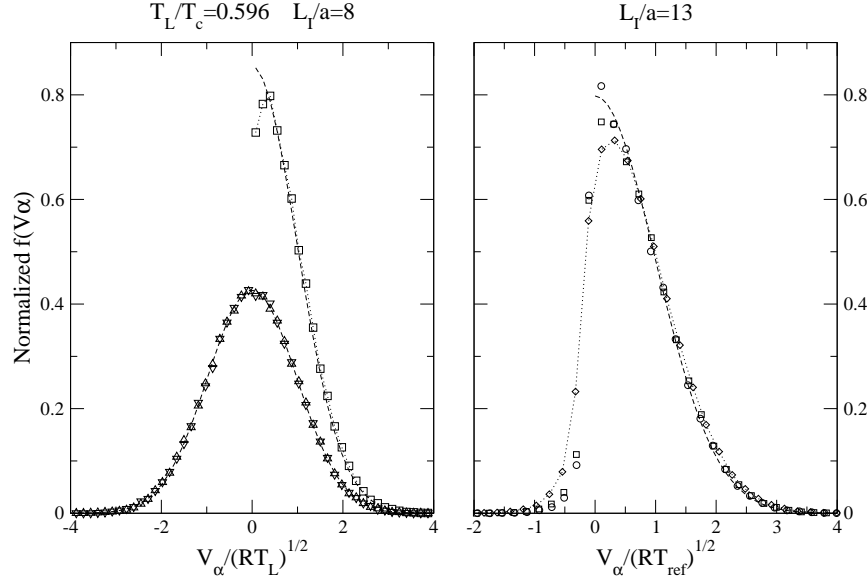


FIGURE 4. (a) Reduced distribution functions of particles absorbed at walls; \square , $f_x(v_x)$; \triangle , $f_y(v_y)$; ∇ , $f_z(v_z)$; dashed line, half and full range Maxwellian at temperature $0.96T_L$; (b) Reduced distribution function $f_x(v_x)$ at $x = x_m$ as a function of T_L ; \circ , $T_L/T_c = 0.596$; \square , $T_L/T_c = 0.663$; \diamond , $T_L/T_c = 0.862$; dashed line, half range Maxwellian with unit temperature. Velocities normalized to $\sqrt{RT_{ref}}$, $T_{ref} = T_\perp(x_m)$.

is possible to estimate it from a simple macroscopic model of the liquid phase. Accordingly, values of the evaporation coefficient σ_e have been computed from the corrected flux \tilde{J}_m using two distinct reference temperatures

$$\sigma_e n_g(T) \sqrt{\frac{RT}{2\pi}} = \tilde{J}_m \quad \left\{ \begin{array}{l} T = T_L \\ T = T_s \end{array} \right. \quad (7)$$

As shown in Fig3(b), the computation of σ_e from T_L leads to a strong temperature dependence of the evaporation coefficient because the evaporation cooling of the slab strongly reduces the evaporation flux. However, if T_s is used, then the temperature variation of the evaporation coefficient is very much reduced and values of σ_e around 0.9 are obtained in all of the cases examined, as also observed in Ref.[8]. As briefly mentioned above, if collisions in the vapor phase could be neglected, then f_e could be reconstructed from the particles absorbed at the walls. Fig.4(a) shows the reduced distribution functions of the velocity component v_x , normal to the walls and of the velocity components v_y and v_z , parallel to the walls, denoted by $f_x(v_x)$, $f_y(v_y)$ and $f_z(v_z)$, respectively. The numerical distribution functions are normalized to unity and compared with a Maxwellian distribution function with zero bulk velocity and a temperature obtained from the v_y and v_z velocity components. It is clear that the distribution functions $f_y(v_y)$ and $f_z(v_z)$ are very well approximated by a Maxwellian, whereas the distribution function $f_x(v_x)$ shows a deviation from the half-range Maxwellian that one would observe if molecules were emitted from the liquid surface according to Eq.(2). The deviation occurs in the low velocity region and it is due to collisions in the vapor phase which preferentially remove slow particles that take a long time to reach the absorbing wall. The effect of temperature on the shape of $f_x(v_x)$ at x_m is described by Fig.4(b). The results show that for small velocity values, a deviation from the local half-range Maxwellian is observed; the difference grows as T_L increases. It should be observed that the velocity distribution functions described above do not take into account the history of individual molecules. As a matter of fact, the positive velocity range of $f_x(v_x)$ at a certain location in the interface region will mostly contain the contribution of molecules originated in the liquid region and travelling toward the vapor phase. However, it will also contain a contribution from vapor molecules which have been reflected back to the vapor phase. The effects of this second molecular group is small, but the deviation from the Maxwellian behavior is also small and it is necessary to check whether the effect is due to the reflected component. To distinguish the two molecular groups a “color” variable has been added to each simulation particle. Particles in the strip $|x| < x_m$ initially get the same “color”. During a simulation, the color variable of a particle is changed only once on entering the vapor region from the interface-vapor boundaries at $\pm x_m$. As expected, the negative tail of the distribution function of molecules which have never crossed the interface-vapor

boundaries is less populated but the shape in the positive velocity range is the same as the full distribution $f_x(v_x)$, indicating that the deviation from Maxwellian behavior is exhibited by the evaporating component and it is not due to the small contribution of the reflected component.

The results described above indicate that, at the boundary between the vapor phase and the interface, the distribution function of evaporating molecules $f_x(v_x)$ deviates to some extent from Eq.(2). Since the deviation is rather limited, it is quite natural to ask whether the vapor motion between the interfaces at $\pm x_m$ and the absorbing walls can be described by the Boltzmann equation with boundary conditions of the kind given by Eqs.(2) and (3). To answer the question a few DSMC simulations have been performed to study the motion of a dilute hard sphere vapor in the gap between x_m and the absorbing wall. The gap width is $L_I - x_m$. The fluid at the left hand side of the interface position has been replaced by a purely diffusive boundary condition ($\alpha = 1$) with $\sigma_e = 0.9$. The saturated vapor density n_w has been taken equal to $n_g(T_s)$ and the wall temperature T_w has been taken initially equal to $T_I(x_m)$ and then adjusted to fit the temperature profiles in the gas phase obtained by the Enskog-Vlasov equation solutions. As is clear, the procedure to match Boltzmann equation to Enskog-Vlasov equation solutions is not rigorous at all. However, the comparison can give an indication of the accuracy of the boundary condition models. Fig.2 shows the comparison of temperatures and velocity profiles in the vapor phase for $T_L/T_c = 0.596$ and $L_I \approx 8a$. This case corresponds to the lowest temperature value where good agreement has been found between $f_x(v_x)$ and a half-range Maxwellian for $v_x > 0$. The temperature profiles obtained by the numerical solution of the Boltzmann equation are in excellent agreement with the Enskog-Vlasov profiles. The velocity profile computed from Boltzmann equation is slightly above the Enskog-Vlasov profile. A closer inspection of the solutions data shows that the discrepancy is due to the negative tail of f_x which, in the Boltzmann equation solution, is less populated than its Enskog-Vlasov counterpart. The comparison of density profiles shows that $n_w = n_g(T_s)$ is a reasonable choice in this particular case. For higher temperature, for which the largest deviation from the half-range Maxwellian has been observed, the agreement is obviously less good.

CONCLUSIONS

The present work is an attempt to give a unified description of a two-phase system through an approximate kinetic equation. The evaporation of a liquid slab into near vacuum is investigated to provide information about the distribution function of molecules emitted from the liquid phase. The non-equilibrium structure of the vapor-liquid interface for various temperature values has been obtained. In particular, the profiles of macroscopic quantities in the transition layer bridging the liquid to the vapor phase has been studied. The examination of reduced distribution functions shows that the velocity component parallel to evaporating surface is very well approximated by a full range Maxwellian. The distribution function of the normal velocity component of outgoing molecules is close to a half-range Maxwellian at the lower values of the investigated temperature range, but deviates from a half-range Maxwellian at higher temperature. These results agree with the recent MD studies of the same problem[12], where a similar behavior of the distribution function has been found in the evaporation of the Lennard-Jones fluid. Therefore, the Enskog-Vlasov model seems to provide a sufficiently realistic description of two-phase flows, in spite of its approximate nature.

REFERENCES

1. Cercignani, C., *Rarefied Gas Dynamics*, Cambridge University Press, Cambridge, 2000.
2. Grmela, M., *J. Stat. Phys.* **3**, 347–364(1971).
3. Karkheck, J., and Stell, G., *J. Chem. Phys.* **75**, 1475–1487(1981).
4. Frezzotti A., Gibelli L., Proceedings of the 23rd International Symposium on Rarefied Gas Dynamics, AIP Conference Proceedings Vol. 663, 980–987 (2003).
5. Tsuruta T., Tanaka H, Masuoka T., *International Journal of Heat and Mass Transfer* **42**, 4107–4116 (1999).
6. Meland R., Frezzotti A., Ytrehus T., Hafskjold B., *Physics of Fluids* **16**, 223–243 (2004).
7. Zhakhovskii V., Anisimov S., *JETP* **84**, 734–745 (1997).
8. Anisimov D., Dunikov S.I., Zhakhovskii V., Malysenko S., *J. Chem. Phys.* **110**, 8722–8729 (1999)
9. Frezzotti, A., *Phys. of Fluids* **9**, 1329–1335 (1997).
10. Allen M.P., Tildesley D.J., *Computer Simulation of Liquids*, Clarendon Press, Oxford, 1987.
11. Resibois P. and DeLeener M., *Classical kinetic theory of fluids*, J. Wiley & Sons, New York, 1997.
12. Ishiyama T., Yano T., Fujikawa S., *Physics of Fluids* **16**, 2899–2906 (2004).